HHS Public Access

Author manuscript

J Biomech. Author manuscript; available in PMC 2019 May 17.

Published in final edited form as:

J Biomech. 2018 May 17; 73: 185–191. doi:10.1016/j.jbiomech.2018.04.010.

Midtarsal locking, the windlass mechanism, and running strike pattern: A kinematic and kinetic assessment

Dustin A. Bruening[a], **Michael B. Pohl**[b], **Kota Z. Takahashi**[c], and **Joaquin A. Barrios**[d]

[a]Brigham Young University, Provo, UT, USA

[b]University of Puget Sound, Tacoma, WA, USA

[c]University of Nebraska at Omaha, Omaha, NE, USA

[d]University of Dayton, Dayton, OH, USA

Abstract

Changes in running strike pattern affect ankle and knee mechanics, but little is known about the influence of strike pattern on the joints distal to the ankle. The purpose of this study was to explore the effects of forefoot strike (FFS) and rearfoot strike (RFS) running patterns on foot kinematics and kinetics, from the perspectives of the midtarsal locking theory and the windlass mechanism. Per the midtarsal locking theory, we hypothesized that the ankle would be more inverted in early stance when using a FFS, resulting in decreased midtarsal joint excursions and increased dynamic stiffness. Associated with a more engaged windlass mechanism, we hypothesized that a FFS would elicit increased metatarsophalangeal joint excursions and negative work in late stance. Eighteen healthy female runners ran overground with both FFS and RFS patterns. Instrumented motion capture and a validated multi-segment foot model were used to analyze midtarsal and metatarsophalangeal joint kinematics and kinetics. During early stance in FFS the ankle was more inverted, with concurrently decreased midtarsal eversion ($p<0.001$) and abduction excursions ($p=0.003$) but increased dorsiflexion excursion ($p=0.005$). Dynamic midtarsal stiffness did not differ ($p=0.761$). During late stance in FFS, metatarsophalangeal extension was increased ($p=0.009$), with concurrently increased negative work ($p<0.001$). In addition, there was simultaneously increased midtarsal positive work ($p<0.001$), suggesting enhanced power transfer in FFS. Clear evidence for the presence of midtarsal locking was not observed in either strike pattern during running. However, the windlass mechanism appeared to be engaged to a greater extent during FFS.

Corresponding Author: Dustin A. Bruening, Exercise Sciences Department, Brigham Young University, 120F RB, Provo, UT 84602, (801) 422-1420, dabruening@gmail.com.

Conflict of interest statement

No conflicts of interest to report

Keywords

rearfoot strike; forefoot strike; multi-segment foot; midfoot; metatarsophalangeal joint

1. INTRODUCTION

Recent research on both injuries and performance during running has focused heavily on comparing foot strike patterns, particularly rearfoot strike (RFS) versus midfoot or forefoot strike (FFS). From an injury management perspective, a FFS has often been advocated due to the associated reductions in vertical ground reaction force (GRF) loading rates (Milner et al., 2006) and elimination of the “impact transient” (De Wit et al., 2000; Laughton et al., 2003; Lieberman et al., 2010). From a mechanical performance-enhancement standpoint, it has been theorized that a FFS could enhance elastic energy storage and return in the Achilles tendon and medial longitudinal arch (MLA) (Ardigo et al., 1995; Divert et al., 2005; Lieberman et al., 2010; Perl et al., 2012).

The influence of strike pattern on both impact forces and mechanical energy profiles is largely related to the coordinated positioning of the lower limb segments in the sagittal plane at initial contact. A FFS pattern places the limb in a position of greater knee flexion and ankle plantarflexion at initial contact, and typically results in a shorter stride and increased cadence (De Wit et al., 2000; Divert et al., 2005; Laughton et al., 2003; Lieberman et al., 2010; Squadrone and Gallozzi, 2009). Studies on lower extremity kinetics have shown differences between strike patterns in mechanical work during stance, with the knee performing greater work in RFS, while the ankle performs more in FFS (De Wit et al., 2000; Hamill et al., 2011; Laughton et al., 2003; Rooney and Derrick, 2013; Stearne et al., 2014; Williams III et al., 2012; Willson et al., 2014). These kinematic and kinetic findings appear independent of whether the strike pattern is habitual or converted (Stearne et al., 2014; Williams et al., 2000), and highlight the large influence strike pattern can have at and above the ankle. However, little is known about the influence of strike pattern on the joints distal to the ankle such as the midtarsal and metatarsophalangeal joints.

An experimental manipulation of strike pattern may also function as a means to further explore two well-known clinical tenets of foot function: the midtarsal locking theory (Elftman, 1960) and the windlass mechanism (Hicks, 1954). The midtarsal locking theory describes a relationship between the subtalar and midtarsal joints such that subtalar inversion skews the oblique and longitudinal axes of the two midtarsal joints, purportedly reducing midtarsal joint mobility. The windlass mechanism states that metatarsophalangeal extension tensions the plantar fascia resulting in concomitant medial longitudinal arch rise, which is thought to be particularly important during late-stance propulsion. Both midtarsal locking and windlass mechanisms are typically assessed using kinematics, but a kinetic analysis may add to our understanding of these theories. In regards to midtarsal locking, previous research shows that a FFS is generally accompanied by a more inverted ankle (Pohl and Buckley, 2008), and thus could alter midfoot dynamic joint stiffness (Davis and DeLuca, 1996). Pertinent to the windlass mechanism, metatarsophalangeal kinematic differences between strike patterns have not been previously reported, but motion could be increased in a FFS

pattern, leading to increased power absorption and negative work done at this joint. A study comparing both kinematics and kinetics of the distal foot joints between strike patterns may provide insight into the nature of these existing theories of foot function during running.

The purpose of the present study was to compare differences in foot kinematics and kinetics between strike patterns during running and explore the extent to which the differences may relate to midtarsal locking and the windlass mechanism. During early stance, we hypothesized that the ankle would be in a more inverted position when using a FFS pattern, thus resulting in decreased midtarsal joint excursions and increased dynamic stiffness, per the midtarsal locking theory. During late stance, we hypothesized that a FFS would elicit increased metatarsophalangeal joint excursions and increased negative work, as related to a more engaged windlass mechanism.

2. METHODS

2.1 Subjects

Eighteen healthy recreational female runners were recruited from a university setting and local running community. All subjects were 18–35 years old and ran at least 16 kilometers per week. Exclusion criteria consisted of any spinal or lower extremity surgery or any knee ligament or cartilage pathology in the past year. Subjects were not recruited based on habitual strike pattern. All subjects gave informed consent as approved by the university's Institutional Review Board. Sample size was estimated using data from a previous study (Pohl and Buckley, 2008). Using the frontal plane ankle and sagittal plane midfoot excursions differences, a required sample size of less than 10 subjects was estimated (80% power).

2.2 Protocol

Subjects were provided New Balance WT10 Minimus shoes with appropriate cut-outs (Shultz and Jenkyn, 2012) so that reflective markers could be placed directly on the skin. Twenty markers were affixed to each subject's pelvis, right thigh, and right shank using clusters to track the thigh and shank motion. Nine markers were placed on the foot through the shoe cut-outs (proximal and distal calcaneus, medial and lateral calcaneus, cuboid, navicular, first and fifth metatarsal heads, and the base of the 2nd metatarsal) (Bruening et al., 2012a). Two additional markers were placed on the shoe approximately over the second metatarsal head and distal phalanges.

Subjects ran along a 20-meter runway at a controlled speed of 3.7 m/s (±5%) (Lieberman et al., 2010). Running speed was monitored using the sacrum marker along the line of progression. Seven successful dynamic trials with the runner's habitual RFS or FFS pattern were collected first, followed by seven trials in the converted condition. Several practice trials were allowed to become familiar with the shoes, running speed, and equipment. For the converted condition, subjects were given a brief demonstration and were verbally instructed to either "run on their toes" or "run on their heels", so that each subject ran with both a RFS and a FFS. Subjects were allowed practice trials with the converted condition as needed, with no subject choosing to utilize more than 4 practice trials. A visual check of the

positioning of the GRF vector at initial contact relative to the tracking foot markers was used to ensure participants landed appropriately during collection. A foot strike index was also calculated post-hoc for comparison purposes. This was defined as the position of the center of pressure (CoP) at initial contact expressed as a percentage of foot length (Cavanagh and Lafortune, 1980). Kinematic data were collected at 150 Hz with an 8-camera motion capture system (Vicon, Oxford Metrics, UK). Force data were collected at 1500 Hz by a floor-mounted force platform (Bertec Corp., Columbus OH, USA).

2.3 Data analysis

Visual 3D software (C-motion Inc., Germantown MD, USA) was used for biomechanical modeling and analysis. A three-segment kinetic foot model was created, modified slightly from Bruening et al. (2012a), containing a rearfoot, mid/forefoot, and phalanges, separated by midtarsal (MT) and metatarsophalangeal (MP) joints. The MT joint center was positioned midway between the cuboid and navicular markers, and the MP joint center midway between the metatarsal heads. Segment positions and orientations were anatomically aligned, and joint angles were not normalized to the standing position.

Marker trajectories from the running trials were low-pass filtered (8 Hz cutoff) along with corresponding force data (50 Hz cutoff). Joint angles were derived using a typical Cardan angle rotation sequence (1-sagittal, 2-frontal, 3-transverse). For kinetics, rigid body inverse dynamics was used to calculate net internal moments and powers at each joint of the foot and lower extremity (Bruening et al., 2012a). To quantify joint moments at the MT and MP joints, we applied inverse dynamics computation only when the CoP was anterior to the respective joint (Stefanyshyn and Nigg, 1997). When the CoP was posterior to the joint, the moments were assumed to be zero. In addition, the unified deformable (UD) modeling approach (Takahashi et al., 2012) was used to calculate the total power of all structures distal to the rearfoot segment. Such analysis includes contributions from both the MT and MP joints, as well as compression of soft tissue or shoe materials.

For each subject, a single trial was chosen for each condition; the trial with the smallest net anterior/posterior impulse was selected to ensure steady state speed throughout stance. Strike patterns were compared using selected metrics as well as entire stance-phase time series waveforms. Metrics consisted of MT and MP joint angular excursions during both early and late stance, the transition being defined by the peak angle near midstance. Note that frontal plane MT motion did not have a prominent peak and excursions were calculated over the same time-period as sagittal plane MT motion. MT angular impulse and stiffness were calculated for the sagittal plane, again over similarly defined early and late stance periods. Stiffness was calculated via the slope of the linear best fit of the moment/angle graph for each stance period. Three frames were cut from either end of each period to reduce non-linear behavior (see Figure 3B). The positive and negative work done at each joint and by the structures distal to the rearfoot, through the UD modeling approach, were also calculated. These metrics were compared between strike patterns using paired t-tests (α = 0.05), and addressed most of the specific hypotheses. To provide additional information on ankle, MT, and MP joint angles, moments, and powers across the entire stance phase, time series waveforms were also analyzed. Note that knee power was included for comparison to

previous studies (Stearne et al., 2014; Williams et al., 2000). Waveforms were first time-normalized to stance and then condition means and standard error (SE) bands were plotted. Mean differences between strike patterns were then plotted with 95% confidence interval (CI) bands. Regions where the CI bands do not cross zero can be considered statistically different ($\alpha = 0.05$). This is an approach that has been simplified from functional data analysis (Andrade et al., 2014).

3. RESULTS

The subject sample demographics for age, height, and weight were: 25 ± 4 yrs., 1.65 ± 0.06 m, 61 ± 7 kg respectively (mean ± stdev). All RFS trials contained strike indices between 0 and 9% (mean ± stdev: 5 ± 3%) while all FFS trials contained strike indices between 53 and 82% (mean ± stdev: 71 ± 7%). These are consistent with contrasting RFS and FFS running patterns (Cavanagh and Lafortune, 1980).

3.1 Kinematics

There were distinct kinematic differences between strike patterns at the ankle in all planes (Figure 1 A–C). During loading response, the ankle was in a more plantarflexed, inverted, and adducted position in FFS. While these differences briefly disappeared around 30% of stance, the ankle quickly returned to a position of greater plantarflexion and inversion (but not adduction) for the remainder of stance.

At the midtarsal joint (Figure 1 D–F, Table 1), the FFS was less inverted and adducted at initial contact. During early stance, FFS resulted in greater MT dorsiflexion excursion ($p=0.005$), but reduced abduction excursion ($p=0.003$). During loading, the direction of the excursion in the frontal plane differed between the strike patterns, with eversion occurring during RFS, and slight inversion during FFS ($p<0.001$). MT angles converged by late stance in all planes. No late stance excursion differences were noted in frontal ($p=0.313$) and transverse planes ($p=0.118$), but there was greater plantarflexion excursion in FFS ($p<0.001$) due to the higher peak dorsiflexion in midstance.

MP joint flexion (Figure 1G, Table 1) was slightly reduced in FFS during early stance ($p=0.009$). During late stance, the MP joint transitioned to extension earlier in FFS and moved through a greater total excursion ($p<0.001$).

3.2 Kinetics

Power profiles at the knee (Figure 2A) and ankle (Figure 2B) showed large differences during early stance, but not late stance. Overall, greater negative work was done by the knee in RFS ($p<0.001$), and by the ankle in FFS ($p<0.001$), with no differences in positive work output by either joint ($p=0.070$ knee, $p=0.376$ ankle).

Sagittal plane MT moments showed that the joint was loaded to a much greater extent in FFS, due to earlier plantarflexion moment onset and greater peak magnitude (Figure 3A), resulting in greater total angular impulse from initial contact to moment peak (RFS = 0.11 ± 0.02 Nm·s/kg, FFS = 0.16 ± 0.02 Nm·s/kg, $p<0.001$). MT power absorption also occurred earlier in FFS (Figure 2C), yet total MT negative work was not different between strike

patterns (p=0.912). Sagittal plane MT joint stiffness (Figure 3B shows a representative subject) was not different during early stance (RFS = 0.41 ± 0.11 Nm/°kg, FFS = 0.40 ± 0.14 Nm/°kg, p=0.761). During late stance, MT angular impulse was again greater in FFS (RFS = 0.11 ± 0.01 Nm·s/kg, FFS = 0.14 ± 0.01 Nm·s/kg, p<0.001). Positive MT joint work was also greater in FFS (p<0.001), concurrent with greater negative work at the MP joint (p<0.001) (Figure 2C–E). Sagittal plane MT joint stiffness did not differ in late stance (RFS = 0.28 ± 0.07 Nm/°kg, FFS = 0.27 ± 0.17 Nm/°kg, p=0.172). A small amount of positive MP joint work was performed just before toe off (80–100% of stance), which was greater in FFS (p<0.001).

The UD foot analysis showed both greater negative and positive work done by the structures distal to the rearfoot in FFS, but these were primarily the result of power differences that were confined to very early (0–10%) and late (80–90%) stance (Figure 3F). In between these regions, the distal-to-rearfoot power closely matched the summation of MP and MT joint power (Figure 2E). Regardless of the foot strike pattern, the foot overall produced greater magnitude of negative work than positive work (Table 1, Figures 2E–F).

4. DISCUSSION

4.1. Early stance

The midtarsal locking theory postulates that subtalar inversion skews the oblique (calcaneocuboid) and longitudinal (talonavicular) joint axes of the midtarsal articulations, resulting in a more rigid midtarsal joint configuration (Elftman, 1960). Conversely, ankle eversion (that typically occurs during early stance) aligns the midtarsal axes in a more parallel configuration, theoretically introducing greater midtarsal mobility. Although our data showed that a FFS running pattern alters these early stance mechanics, only partial support was found for the presence of a midtarsal locking mechanism. In agreement with previous studies (Peters et al., 2017; Pohl and Buckley, 2008; Williams et al., 2000), we observed that the ankle was more inverted throughout stance in FFS running (Figure 1B), which should theoretically increase the locking effect at the midtarsal joint. However, the additional ankle inversion seen in FFS was only 5 degrees at initial contact, and converged to around 1 degree shortly afterwards. Consequently, we noted some effects that may be related to midtarsal locking function, but these were quite modest. In the frontal plane, MT eversion excursion was seen in RFS, while only minimal deviations in MT position were seen in FFS (Figure 1E). The transverse plane kinematic data also showed evidence of a mild locking effect, as slightly less abduction excursion was seen in FFS. Conversely, however, in the sagittal plane we saw an increased dorsiflexion excursion in FFS. While this may appear to conflict with kinematic-based locking, the additional dorsiflexion motion in FFS corresponded with an increased MT plantarflexion moment (Figure 3A).

While the midtarsal locking theory has typically been evaluated using kinematic analyses (Blackwood et al., 2005; Elftman, 1960; Okita et al., 2014), the inclusion of MT joint kinetics in the current study provided additional insight. For instance, early stance dynamic joint stiffness was expected to be greater in FFS. However, no differences were seen. It appears that the MT moment and associated angular excursion both increased proportionally in FFS. It is possible that the small increase in FFS ankle inversion was insufficient to

functionally “lock” the MT joint in the sagittal plane (Youberg et al., 2005). Further, because the stiffness calculation was limited to the sagittal plane, it may not fully reflect the tri-planar nature of MT joint stiffening, as some evidence of locking was noted in other planes. We should also note that the midtarsal moment/angle plots exhibited substantial variability and some non-linear behavior, both of which could be due to differences in foot structure or the combination of active and passive tissues inherent in the midtarsal joint.

The joint power profiles provide additional insight into foot mechanics during running, particularly when looking across both the MT and MP joints. The MT joint began absorbing power earlier in FFS, with greater power absorption through most of early stance (Figure 2C). This finding is suggestive of increased eccentric demand to the intrinsic foot muscles that cross the MT joint, supporting recent findings of foot intrinsic hypertrophy in individuals who utilize non-RFS patterns due to minimalist shoe use (Miller et al., 2014). The initiation of power absorption at the MP joint also occurred earlier in FFS. Taken together (Figure 2E), combined MT and MP power absorption is increased through approximately 40% of stance in FFS. At this instant, the combined MT and MP power profiles converged, despite marked differences in the individual MT and MP joint contributions. This convergence may be associated in part with the windlass mechanism, as the onset of MP extension motion also occurs at this point (Figure 1G).

4.2. Late stance

The midtarsal locking theory purports that the oblique and longitudinal midtarsal axes become more skewed as the ankle inverts in late stance, supposedly locking the midfoot and allowing the whole foot to act as a rigid lever for push off (Elftman, 1960). However, our results do not support the presence of a locked or rigid midfoot, as a substantial amount of plantarflexion and positive work occurred at the MT joint during late stance regardless of strike pattern. This kinematic pattern matches previous observations made during walking and running (e.g. (Bruening et al., 2012b; Pohl and Buckley, 2008; Pohl et al., 2007)) as well as in cadaveric simulations (Okita et al., 2014). In addition, MT stiffness was approximately 32% lower in late stance than in early stance, suggesting that the joint was actually more compliant in late stance. Comparing strike patterns in the present study, there were minimal differences in MT kinematics (Figure 1 D–F) between strike patterns and no difference in MT joint stiffness in late stance, despite increased ankle inversion throughout late stance in FFS. Overall, the term “locking” does not appear appropriate to describe the midtarsal joints during late stance.

In contrast, the windlass mechanism does appear to have a strong influence on late stance mechanics. This mechanism (Hicks, 1954) views the plantar aponeurosis as a continuous fascial structure connecting the calcaneus with the proximal phalanges. As the MP joint extends, it supposedly exerts a force on the calcaneus in a manner similar to a mechanical windlass, acting to shorten the foot and raise the MLA. Indeed, our data shows that MP extension begins earlier and moves through a greater excursion in FFS (Figure 1G). Further, peak MT dorsiflexion occurred earlier and was greater in FFS. This combination of altered MT and MP joint motions suggest earlier and likely greater tensile loading of the plantar fascia in FFS.

Several additional insights into the role of the windlass mechanism were gained by examining the combined MT and MP joint kinetics. First, it appears that during running the windlass mechanism transfers power between the two joints, as power generation at the MT joint occurred concurrently with power absorption at the MP joint (see also (Bruening et al., 2012a; McDonald et al., 2016; Wager and Challis, 2016)). Second, a FFS magnifies the power transfer effect of the windlass mechanism; a FFS resulted in similar increases in both negative MP work and positive MT work. When accounting for these simultaneous effects, the combined MT and MP power was not different between strike patterns through most of late stance (Figure 2E), reinforcing the idea that the windlass mechanism redistributes some of the energy absorbed by MP extension (McDonald et al., 2016; Stefanyshyn and Nigg, 1997; Wager and Challis, 2016). Third, potentially due to this more engaged windlass mechanism during mid-to-late stance, FFS produced slightly greater distal-to-rearfoot positive work prior to toe-off (~ last 20% of stance). We speculate that this enhanced push-off work could arise from either energy return from elastic structures (such as the plantar fascia) or increased activation from the intrinsic and extrinsic muscles (Miller et al., 2014). Further investigation involving intramuscular electromyography (Kelly et al., 2016) and musculoskeletal modeling (McDonald et al., 2016; Wager and Challis, 2016) is needed to reconcile the exact source of the foot work production.

Regardless of the running strike patterns, it is interesting to note that the foot overall produced greater magnitude of negative work than positive work. Although foot mechanics during running is thought to harness the elasticity of the plantar fascia (Alexander et al., 1987; McDonald et al., 2016; Wager and Challis, 2016), our results showed that the foot is not entirely elastic, but rather it also contains viscoelastic elements that absorb mechanical energy (Takahashi et al., 2017).

4.3 Limitations

Our study methodology involved a few assumptions. First, we did not control for habitual strike pattern nor evaluate any potential adaptations that may occur as subjects acutely convert strike pattern. We based this decision on previous studies showing strong similarities between habitual and converted strike patterns (Stearne et al., 2014; Williams et al., 2000), even with minimal practice. This assumption allowed us to design a within-subjects study to evaluate mechanics due entirely to changes in limb positioning. Second, our multi-segment foot modeling approach relied on rigid body assumptions as well as ground reaction forces partitioned from a single force platform. Similar methodology has been used in previous studies (Firminger and Edwards, 2016; McDonald et al., 2016; Stefanyshyn and Nigg, 1997), however, a gold standard for validation has not been established. The simultaneous use of the deformable foot methodology revealed similar conclusions as the combined MT and MP joint powers, thus giving additional support that the strike patterns altered the mechanical work profiles within the foot.

5. CONCLUSIONS

Overall, there was only modest support for an increased midtarsal locking effect in FFS, evidenced by decreased motion in frontal and transverse plane MT kinematics. However,

there were no differences in sagittal plane MT dynamic stiffness despite increases in sagittal plane MT moments in FFS. There was increased negative work done in early stance in FFS, which may indicate additional eccentric muscle demand or passive forefoot deformation. The large amount of sagittal plane MT motion that occurred during late stance suggests that the midfoot was not “locked”, regardless of strike pattern. Instead, the greater MT positive power in the FFS during late stance is likely the result of a more engaged windlass mechanism. Evidence of this is provided by earlier and greater MP extension occurring in FFS, and also greater transfer of negative MP power to positive MT power. In running, clear evidence for the presence of midtarsal locking was not observed in either strike pattern. However, a more engaged windlass mechanism was evident in FFS.

References

Alexander R, Ker R, Bennet M, Bibby S, Kester R. The spring in the arch of the human foot. Nature. 1987; 325:147–149. [PubMed: 3808070]

Andrade AG, Polese JC, Paolucci LA, Menzel H-JK, Teixeira-Salmela LF. Functional data analyses for the assessment of joint power profiles during gait of stroke subjects. Journal of applied biomechanics. 2014:30.

Ardigo L, Lafortuna C, Minetti A, Mognoni P, Saibene F. Metabolic and mechanical aspects of foot landing type, forefoot and rearfoot strike, in human running. Acta Physiologica Scandinavica. 1995; 155:17–22. [PubMed: 8553873]

Blackwood CB, Yuen TJ, Sangeorzan BJ, Ledoux WR. The midtarsal joint locking mechanism. Foot & ankle international. 2005; 26:1074–1080. [PubMed: 16390642]

Bruening DA, Cooney KM, Buczek FL. Analysis of a kinetic multi-segment foot model part II: kinetics and clinical implications. Gait & posture. 2012a; 35:535–540. [PubMed: 22197290]

Bruening DA, Cooney KM, Buczek FL. Analysis of a kinetic multi-segment foot model. Part I: Model repeatability and kinematic validity. Gait & posture. 2012b; 35:529–534. [PubMed: 22421190]

Cavanagh PR, Lafortune MA. Ground reaction forces in distance running. Journal of biomechanics. 1980; 13:397–406. [PubMed: 7400169]

Davis RB, DeLuca PA. Gait characterization via dynamic joint stiffness. Gait & Posture. 1996; 4:224–231.

De Wit B, De Clercq D, Aerts P. Biomechanical analysis of the stance phase during barefoot and shod running. Journal of biomechanics. 2000; 33:269–278. [PubMed: 10673110]

Divert C, Mornieux G, Baur H, Mayer F, Belli A. Mechanical comparison of barefoot and shod running. International journal of sports medicine. 2005; 26:593–598. [PubMed: 16195994]

Elftman H. The transverse tarsal joint and its control. Clinical orthopaedics. 1960; 16:41. [PubMed: 13819895]

Firminger CR, Edwards WB. The influence of minimalist footwear and stride length reduction on lower-extremity running mechanics and cumulative loading. Journal of Science and Medicine in Sport. 2016

Hamill J, Russell EM, Gruber AH, Miller R. Impact characteristics in shod and barefoot running. Footwear Science. 2011; 3:33–40.

Hicks J. The mechanics of the foot: II. The plantar aponeurosis and the arch. Journal of anatomy. 1954; 88:25. [PubMed: 13129168]

Kelly LA, Lichtwark GA, Farris DJ, Cresswell A. Shoes alter the spring-like function of the human foot during running. Journal of The Royal Society Interface. 2016; 13:20160174.

Laughton CA, Davis I, Hamill J. Effect of strike pattern and orthotic intervention on tibial shock during running. Journal of Applied Biomechanics. 2003; 19:153–168.

Lieberman DE, Venkadesan M, Werbel WA, Daoud AI, D’Andrea S, Davis IS, Mang’Eni RO, Pitsiladis Y. Foot strike patterns and collision forces in habitually barefoot versus shod runners. Nature. 2010; 463:531–535. [PubMed: 20111000]

McDonald KA, Stearne SM, Alderson JA, North I, Pires NJ, Rubenson J. The role of arch compression and metatarsophalangeal joint dynamics in modulating plantar fascia strain in running. PloS one. 2016; 11:e0152602. [PubMed: 27054319]

Miller EE, Whitcome KK, Lieberman DE, Norton HL, Dyer RE. The effect of minimal shoes on arch structure and intrinsic foot muscle strength. Journal of Sport and Health Science. 2014; 3:74–85.

Milner CE, Ferber R, Pollard CD, Hamill J, Davis IS. Biomechanical factors associated with tibial stress fracture in female runners. Medicine & Science in Sports & Exercise. 2006; 38:323–328. [PubMed: 16531902]

Okita N, Meyers SA, Challis JH, Sharkey NA. Midtarsal joint locking: new perspectives on an old paradigm. Journal of Orthopaedic Research. 2014; 32:110–115. [PubMed: 24038197]

Perl DP, Daoud AI, Lieberman DE. Effects of footwear and strike type on running economy. Med Sci Sports Exerc. 2012; 44:1335–1343. [PubMed: 22217565]

Peters H, Deschamps K, Matricali GA, Staes F. Foot segmental mobility during subphases of running: Comparative study between two striking patterns. Gait & Posture. 2017; 53:127–130. [PubMed: 28157573]

Pohl MB, Buckley JG. Changes in foot and shank coupling due to alterations in foot strike pattern during running. Clinical Biomechanics. 2008; 23:334–341. [PubMed: 18006125]

Pohl MB, Messenger N, Buckley JG. Forefoot, rearfoot and shank coupling: effect of variations in speed and mode of gait. Gait & posture. 2007; 25:295–302. [PubMed: 16759862]

Rooney BD, Derrick TR. Joint contact loading in forefoot and rearfoot strike patterns during running. Journal of Biomechanics. 2013; 46:2201–2206. [PubMed: 23910541]

Shultz R, Jenkyn T. Determining the maximum diameter for holes in the shoe without compromising shoe integrity when using a multi-segment foot model. Medical engineering & physics. 2012; 34:118–122. [PubMed: 21890394]

Squadrone R, Gallozzi C. Biomechanical and physiological comparison of barefoot and two shod conditions in experienced barefoot runners. Journal of Sports Medicine and Physical Fitness. 2009; 49:6. [PubMed: 19188889]

Stearne SM, Alderson JA, Green BA, Donnelly CJ, Rubenson J. Joint kinetics in rearfoot versus forefoot running: implications of switching technique. Med Sci Sports Exerc. 2014; 46:1578–1587. [PubMed: 24500531]

Stefanyshyn DJ, Nigg BM. Mechanical energy contribution of the metatarsophalangeal joint to running and sprinting. Journal of biomechanics. 1997; 30:1081–1085. [PubMed: 9456374]

Takahashi KZ, Kepple TM, Stanhope SJ. A unified deformable (UD) segment model for quantifying total power of anatomical and prosthetic below-knee structures during stance in gait. Journal of biomechanics. 2012; 45:2662–2667. [PubMed: 22939292]

Takahashi KZ, Worster K, Bruening DA. Energy neutral: the human foot and ankle subsections combine to produce near zero net mechanical work during walking. Scientific Reports. 2017; 7:15404. [PubMed: 29133920]

Wager JC, Challis JH. Elastic energy within the human plantar aponeurosis contributes to arch shortening during the push-off phase of running. Journal of biomechanics. 2016; 49:704–709. [PubMed: 26944691]

Williams DS, McClay IS, Manal KT. Lower extremity mechanics in runners with a converted forefoot strike pattern. Journal of Applied Biomechanics. 2000; 16:210–218.

Williams DB III, Green DH, Wurzinger B. Changes in lower extremity movement and power absorption during forefoot striking and barefoot running. International journal of sports physical therapy. 2012; 7:525. [PubMed: 23091785]

Willson JD, Bjorhus JS, Williams DB, Butler RJ, Porcari JP, Kernozek TW. Short-term changes in running mechanics and foot strike pattern after introduction to minimalistic footwear. PM&R. 2014; 6:34–43. [PubMed: 23999160]

Youberg LD, Cornwall MW, McPoil TG, Hannon PR. The amount of rearfoot motion used during the stance phase of walking. Journal of the American Podiatric Medical Association. 2005; 95:376–382. [PubMed: 16037554]

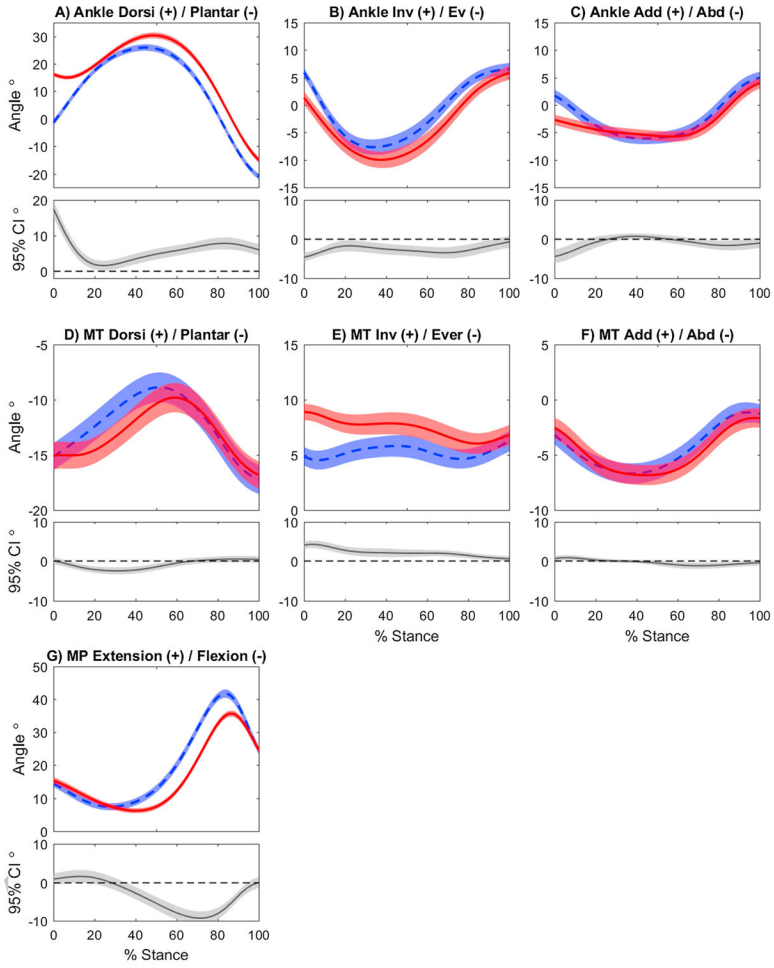

Figure 1.

Ankle, midtarsal (MT), and metatarsophalangeal (MP) joint angles, time normalized across stance phase (0–100%) for rearfoot (RFS) and forefoot (FFS) strike patterns. Each curve contains the mean ± standard error bands (shaded regions). Below each angle plot is a between-condition difference plot (RFS - FFS), containing the mean ± 95% confidence interval bands. Regions where those bands separate from zero can be considered regions of statistical differences. (Legend: – – FFS, ——RFS)

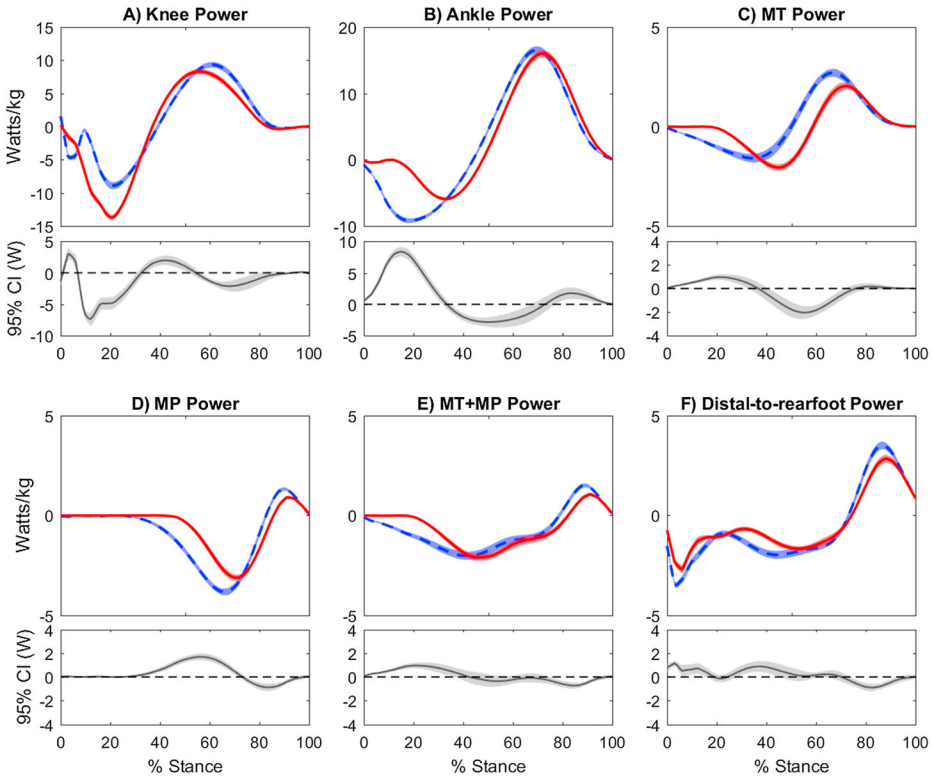

Figure 2.

Power profiles for the knee, ankle, midtarsal (MT), and metatarsophalangeal (MP) joints as well as for the structures distal to the rearfoot for rearfoot (RFS) and forefoot (FFS) strike patterns. Each curve contains the mean and ± standard error bands (shaded regions). Below each angle plot is a within-subject difference plot (RFS - FFS), containing the mean ± 95% confidence interval bands. Where those bands separate from zero can be roughly considered regions of statistical differences. (Legend: – – FFS, —— RFS)

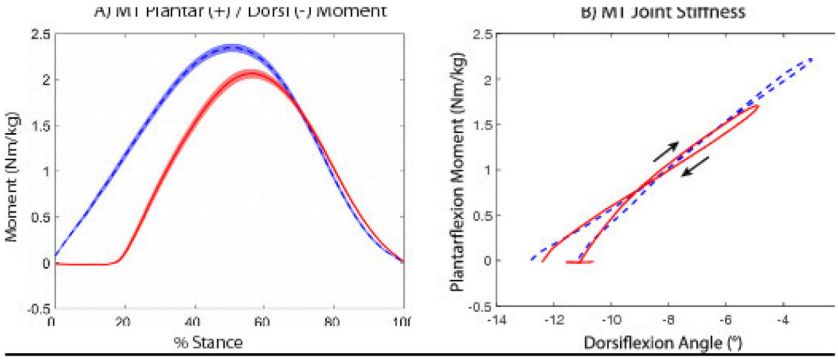

Figure 3.

Sagittal plane midtarsal (MT) moment and stiffness for rearfoot (RFS) and forefoot (FFS) strike patterns. A) Sagittal plane MT moment across stance phase (mean ± standard error bands as in Figure 1). B) Sagittal plane MT moment vs angle plot for a single representative subject. Stiffness was calculated as a linear best fit during early (moving upward and right in this subject) and late stance (moving downward and left). Note that the beginning of the RFS plot is horizontal until the CoP passes anterior to the MT joint; this portion was not included in the RFS stiffness. (Legend: – – FFS, —— RFS)

Table 1

Midtarsal (MT) and metatarsophalangeal (MP) joint excursions (mean ± standard deviation) during early and late stance for rearfoot (RFS) and forefoot (FFS) strike patterns.

	Early Stance			Late Stance		
	RFS	**FFS**	**p-value**	**RFS**	**FFS**	**p-value**
MT Dorsi (+)/Plantar (−)	5.4 ± 1.5	6.4 ± 2.2	*0.005	−7.1 ± 1.7	−8.5 ± 2.2	*<0.001
MT Inv (+)/Ev (−)	−3.0 ± 1.3	2.2 ± 1.6	*<0.001	−2.1 ± 1.4	−2.5 ± 1.8	0.313
MT Add (+)/Abd (−)	−4.5 ± 1.2	−3.7 ± 1.2	*0.003	4.8 ± 1.5	5.2 ± 1.9	0.118
MP Ext (+)/Flex (−)	−9.3 ± 2.4	−7.2 ± 2.8	*0.009	30.0 ± 3.2	34.8 ± 2.9	*<0.001

*Statistically significant at $\alpha = 0.05$.

J Biomech. Author manuscript; available in PMC 2019 May 17.

Table 2

Positive and negative joint work done at the knee, ankle, midtarsal (MT), and metatarsophalangeal (MP) joints, as well as by structures distal to the rearfoot for rearfoot (RFS) and forefoot (FFS) strike patterns.

	Negative Work (J/kg)			Positive Work (J/kg)		
	RFS	**FFS**	**p-value**	**RFS**	**FFS**	**p-value**
Knee	−0.63±0.11	−0.42±0.12	*<0.001	0.54±0.09	0.57±0.11	0.070
Ankle	−0.29±0.06	−0.58±0.10	*<0.001	1.04±0.12	1.07±0.14	0.376
MT	−0.11±0.03	−0.11±0.05	0.912	0.09±0.04	0.15±0.04	*<0.001
MP	−0.16±0.04	−0.23±0.05	*<0.001	0.02±0.01	0.03±0.01	*<0.001
Distal-to-rearfoot	−0.21±0.04	−0.27±0.07	*0.007	0.11±0.04	0.13±0.04	*0.008

*Statistically significant at $\alpha = 0.05$.